

Coherent oscillations in a superconducting tunable flux qubit manipulated without microwaves

S. Poletto¹, F. Chiarello², M. G. Castellano², J. Lisenfeld¹, A. Lukashenko¹, C. Cosmelli³, G. Torrioli², P. Carelli⁴ and A. V. Ustinov^{1*}
¹ *Physikalisches Institut, Universität Karlsruhe (TH), D-76131 Karlsruhe, Germany*
² *Istituto di Fotonica e Nanotecnologie, CNR, 00156 Roma, Italy*
³ *Dip. Fisica, Università di Roma La Sapienza, 00185 Roma, Italy*
⁴ *Dip. Ingegneria Elettrica, Università dell'Aquila, 67040 Monteluco di Roio, Italy*
(Dated: November 2, 2018)

We experimentally demonstrate the coherent oscillations of a tunable superconducting flux qubit by manipulating its energy potential with a nanosecond-long pulse of magnetic flux. The occupation probabilities of two persistent current states oscillate at a frequency ranging from 6 GHz to 21 GHz, tunable via the amplitude of the flux pulse. The demonstrated operation mode allows to realize quantum gates which take less than 100 ps time and are thus much faster compared to other superconducting qubits. An other advantage of this type of qubit is its insensitivity to both thermal and magnetic field fluctuations.

PACS numbers: 03.67.Lx, 85.25.Dq

Superconducting qubits stand between the most promising systems for the realization of quantum computation. Coherent quantum evolution and manipulation have been demonstrated and extensively studied for single [1, 2, 3, 4, 5] and coupled superconducting qubits [6, 7, 8, 9, 10, 11]. In most cases, the state of superconducting qubits are manipulated by means of microwave pulses, with a technique similar to the NMR manipulation of atoms. An alternative way to manipulate qubits is based on modifying their energy potential without applying any microwave signals [1, 5]. The latter approach requires a much simpler experimental technique and offers the possibility of using classical logic signals to control a quantum processor *in situ*, which is advantageous for the large scale implementation of a quantum circuits.

In this Letter, we report the observation of tunable coherent oscillations in a SQUID-based flux qubit. These oscillations are obtained by manipulating the qubit with nanosecond-long pulses of magnetic flux rather than microwaves. By this technique, we could increase the oscillation frequency up to 21 GHz, which allows to perform very fast logical quantum gates. Since the relevant quality factor of a qubit is the number of gate operations which can be performed during its coherence time, this result is of particular interest towards the realization of a solid-state quantum computer.

The investigated circuit, shown in Fig. 1(a), is a double SQUID consisting of a superconducting loop of inductance $L = 85$ pH, interrupted by a small dc SQUID of loop inductance $l = 6$ pH. This dc SQUID is operated as a single Josephson junction (JJ) whose critical current is tunable by an external magnetic field. Each of the two JJs embedded in the dc SQUID has a critical current $I_0 = 8\mu\text{A}$ and capacitance $C = 0.4$ pF. The qubit is manipulated by changing two magnetic fluxes Φ_x and Φ_c , applied to the large and small loops by means of two coils

of mutual inductance $M_x = 2.6$ pH and $M_c = 6.3$ pH, respectively. The readout of the qubit flux is performed by measuring the switching current of an unshunted dc SQUID, which is inductively coupled to the qubit [12]. The circuit was manufactured by Hypres [13] using standard Nb/AlO_x/Nb technology in a 100 A/cm² critical current density process. The dielectric material used for junction isolation is SiO₂. The whole circuit is designed gradiometrically in order to reduce magnetic flux pick-up and spurious flux couplings between the loops. The JJs have dimensions of $3 \times 3\mu\text{m}^2$ and the entire device occupied a space of $230 \times 430\mu\text{m}^2$. All the measurements have been performed at a sample temperature of 15 mK. The currents generating the two fluxes Φ_x and Φ_c were supplied via coaxial cables including 10 dB attenuators at the 1K-pot stage of a dilution refrigerator. To generate the flux Φ_c , a bias-tee at room temperature was used to combine the outputs of a current source and a pulse generator. For biasing and sensing the readout dc SQUID, we used superconducting wires and metal powder filters [14] at the base temperature, as well as attenuators and low-pass filters with a cut-off frequency of 10 kHz at the 1K-pot stage. The chip holder with the powder filters was surrounded by one superconducting and two cryoperm shields.

Assuming identical junctions and negligible inductance of the smaller loop ($l \ll L$), the system dynamics is equivalent to the motion of a particle with the Hamiltonian

$$H = \frac{p^2}{2M} + \frac{\Phi_b^2}{L} \left[\frac{1}{2}(\varphi - \varphi_x)^2 - \beta(\varphi_c) \cos \varphi \right],$$

where $\varphi = \Phi/\Phi_b$ is the spatial coordinate of the equivalent particle, p is the relative conjugate momentum, $M = C\Phi_b^2$ is the effective mass, $\varphi_x = \Phi_x/\Phi_b$ and $\varphi_c = \pi\Phi_c/\Phi_0$ are the normalized flux controls, and

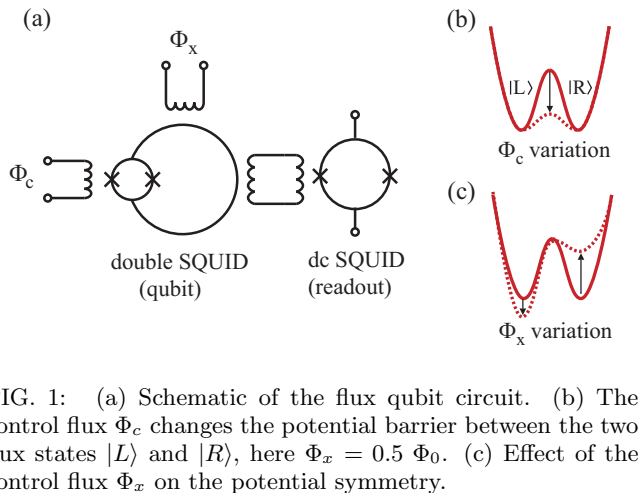


FIG. 1: (a) Schematic of the flux qubit circuit. (b) The control flux Φ_c changes the potential barrier between the two flux states $|L\rangle$ and $|R\rangle$, here $\Phi_x = 0.5 \Phi_0$. (c) Effect of the control flux Φ_x on the potential symmetry.

$\beta(\varphi_c) = (2I_0L/\Phi_b) \cos \varphi_c$, with $\Phi_0 = h/(2e)$ and $\Phi_b = \Phi_0/(2\pi)$. For $\beta < 1$ the potential has a single minimum, otherwise it consists of multiple wells. In the particular case of $1 < \beta < 4.6$ and $\Phi_x = \Phi_0/2$, the system potential is a symmetric double well shown in Fig. 1(b). The two states $|L\rangle$ and $|R\rangle$, which are respectively localized in the left and right potential well, correspond to a persistent current circulating either clockwise or counter-clockwise in the main SQUID loop. As it is shown in Fig. 1(b), the external flux Φ_c controls the height of the barrier separating the minima, while a variation of Φ_x changes the symmetry of the potential as indicated in Fig. 1(c). In this work, we exploit both the double well and the single well properties. The double well potential shape is used for qubit initialization and readout. The single well, or more exactly the two lowest energy states $|0\rangle$ and $|1\rangle$ in this well, is used for the coherent evolution of the qubit.

We use a well established procedure [15] to identify the regions where the system has a double well potential in the $\Phi_c - \Phi_x$ plane. The flux response Φ of the qubit is measured as a function of Φ_x and Φ_c fluxes and the switching points between different flux states are detected. Figure 2(a) shows $\Phi - \Phi_x$ characteristics obtained for two Φ_c values using initial state preparation in different wells. One can easily identify here a bi-stability region in the vicinity of $\Phi_x \approx 0.5 \Phi_0$ and a mono-stability region outside the hysteretic curve, corresponding to the presence of a double and a single potential well, respectively. At the border between these regions we find abrupt switching between the two stable states. The positions Φ_x of the switching points are plotted in Fig. 2(b) for different Φ_c values. This diagram allows to easily identify the combinations of parameters resulting in a single- or double-well potential. A single-well region is found for $\Phi_c \gtrsim 0.42$.

The measurement process that we used to observe coherent oscillations consists of several steps shown in Fig. 3(a). Each step is realized by applying a combination of magnetic fluxes Φ_x and Φ_c as indicated by num-

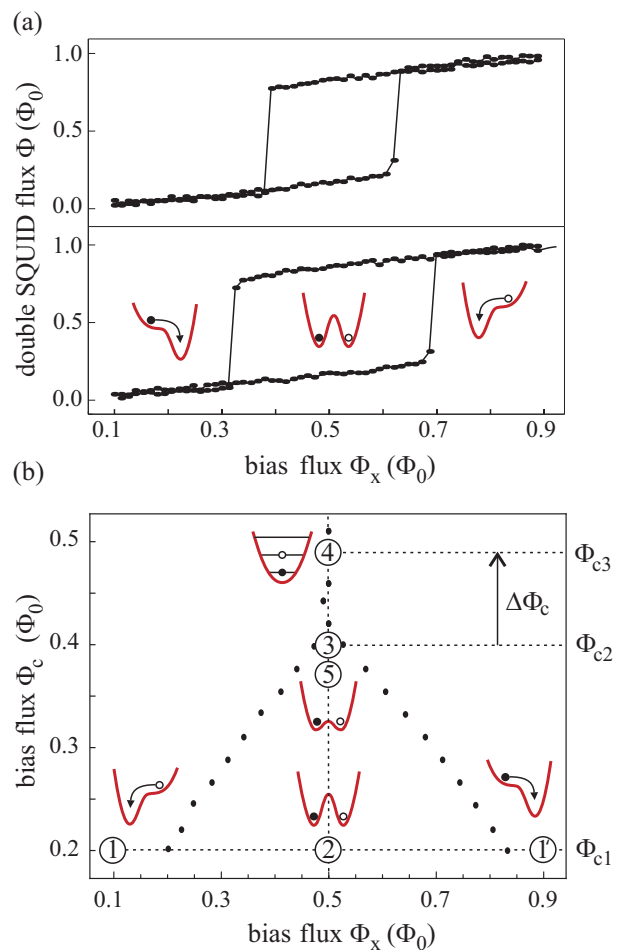


FIG. 2: (a) The measured double SQUID flux Φ in dependence of Φ_x , plotted for two different values of Φ_c and initial preparation in either potential well. (b) Position of the switching points (dots) in the $\Phi_c - \Phi_x$ parameter space. Numbered tags indicate the working points for qubit manipulation at which the qubit potential has a shape as indicated in the insets.

bers in Fig. 2(b). The first step in our measurement is the initialization of the system in a defined flux state (1). Starting from a double well at $\Phi_x \cong \Phi_0/2$ with high barrier, the potential is tilted by changing Φ_x until it has only a single minimum (left or right, depending on the amplitude and polarity of the applied flux pulse). This potential shape is maintained long enough to ensure the relaxation to the ground state. Afterwards the potential is tuned back to the initial double-well state (2). The high barrier prevents any tunneling and the qubit is thus initialized in the chosen potential well. Next, the barrier height is lowered to an intermediate level (3) that preserves the initial state and allows to use just a small-amplitude Φ_c flux pulse for the subsequent manipulation. The following Φ_c -pulse transforms the potential into a single well (4). The Φ_c -pulse duration Δt is in the nanosecond range. The relative phase of the ground and

the first excited states evolves depending on the energy difference between them. Once Φ_c -pulse is over, the double well is restored and the system is measured in the basis $\{|L\rangle, |R\rangle\}$ (5). The readout of the qubit flux state is done by applying a bias current ramp to the dc SQUID and recording its switching current to the voltage state.

The pattern that realizes the above described manipulation is reported in Fig. 3(b). The flux Φ_x is switched between two values: Φ_{x2} is used to create a strongly asymmetric potential for qubit initialization in the left or right well, and Φ_{x1} equal to $\Phi_0/2$ (or very close to it) transforms the potential into a symmetric (or nearly symmetric) double well. The flux Φ_c is changed between three different values: Φ_{c1} and Φ_{c2} define, respectively, high and intermediate amplitudes of the barrier between the two minima, while at $\Phi_{c3} = \Phi_{c2} + \Delta\Phi_c$ the barrier is removed completely and the potential turns into a single well. The amplitude $\Delta\Phi_c$ of the pulse is varied allowing for single wells of different curvature at the bottom. The nominal rise and fall times of this pulse are $t_{r/f} = 0.6$ ns.

The flux pattern is repeated for $10^2 - 10^4$ times in order to evaluate the probability $P_L = |\langle L | \Psi_{\text{final}} \rangle|^2$ of occupation of the left state at the end of the manipulation. By changing the duration Δt of the manipulation pulse Φ_c , we observed coherent oscillations between the occupations of the states $|L\rangle$ and $|R\rangle$ shown in Fig. 4(a). The oscillation frequency could be tuned between 6 and 21 GHz by changing the pulse amplitude $\Delta\Phi_c$. These oscillations persist when the potential is made slightly asymmetric by varying the value Φ_{x1} . As it is shown in Fig. 4(b), detuning from the symmetric potential by up to $\pm 2.9\text{m}\Phi_0$ only slightly changes the amplitude and symmetry of the oscillations. When the qubit was initially prepared in $|R\rangle$ state instead of $|L\rangle$ state we observed similar oscillations.

To understand the physical process behind the observed oscillations, let us discuss in detail what happens during the manipulation. Suppose the system is initially prepared in the left state $|L\rangle$ of a perfectly symmetric double well potential. During the Φ_c pulse, the potential has only one central minimum and can be approximated by a harmonic oscillator potential with frequency $\omega_0(\Phi_{c3}) \approx 1/\sqrt{2LC} \sqrt{1 - \beta(\Phi_{c3})}$. The pulse transforms the initially prepared left state (that is a symmetric superposition of the two lowest energy eigenstates of the double well potential $|\tilde{0}\rangle$ and $|\tilde{1}\rangle$, i.e. $|L\rangle = (|\tilde{0}\rangle + |\tilde{1}\rangle)/\sqrt{2}$) into the superposition of the two lowest energy eigenstates $|0\rangle$ and $|1\rangle$ of the single-well potential. To achieve that, the pulse rise time needs to be shorter than the relaxation time but, at the same time, long enough to avoid population of upper energy levels. During the plateau of the $\Delta\Phi_c$ pulse, the relative phase θ between the states $|0\rangle$ and $|1\rangle$ evolves with time at the Larmor frequency given by $\omega_0 = (E_1 - E_0)/\hbar$. At the end of the pulse the accumulated relative phase becomes $\theta = \omega_0 \Delta t$. Turning the system back into the

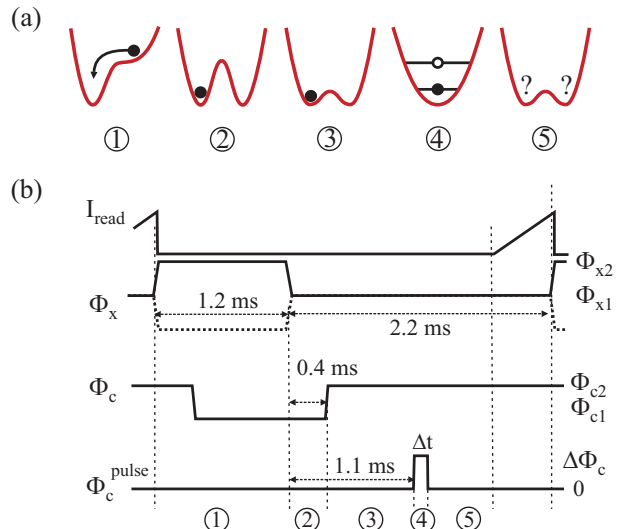


FIG. 3: (a) Variation of the potential shape during the manipulation. (b) Time sequence of the readout dc SQUID current (topmost line) and flux bias values (bottom lines).

double-well maps the phase to the two flux states $|L\rangle$ and $|R\rangle$. The final state after the flux pulse Φ_c is $|\Psi_{\text{final}}\rangle = \cos(\theta/2) |L\rangle + i \sin(\theta/2) |R\rangle$. Note that in the more realistic case of non perfectly symmetric double-well potential, the initial left state is no more a symmetric superposition, but tends more to either $|\tilde{0}\rangle$ or $|\tilde{1}\rangle$ due to the potential unbalancing. However, a pulse with a short rise time induces a non-adiabatic transition that populates mainly the two lowest energy eigenstates $|0\rangle$ and $|1\rangle$ in the single well potential. This condition can be met in a narrow region of the flux bias plane called “portal” [16]. This non-adiabatic transition also leads to the phase evolution process described above.

In order to verify above interpretation, we numerically solved the time-dependent Schrödinger equation for this system. The simulation showed that with our experimental parameters the transition between the first two levels occurs as described, while the occupation of upper levels remains below few percents.

The oscillation frequency ω_0 depends on the amplitude of the manipulation pulse $\Delta\Phi_c$ since it determines the shape of the single well potential and the energy level spacing $E_1 - E_0$. A pulse of larger amplitude $\Delta\Phi_c$ generates a deeper well having a larger level spacing, which leads to a larger oscillation frequency as shown in Fig. 4(a). In Fig. 5, we plot the energy spacing between the ground state and the three excited states (indicated as $(E_k - E_0)/\hbar$ with $k=1,2,3$) versus the flux $\Phi_{c3} = \Phi_{c2} + \Delta\Phi_c$ obtained from a numerical simulation of our system using the experimental parameters. In the same figure, we plot the measured oscillation frequencies for different values of Φ_c (open circles). Excellent agreement between simulation (solid line) and data strongly

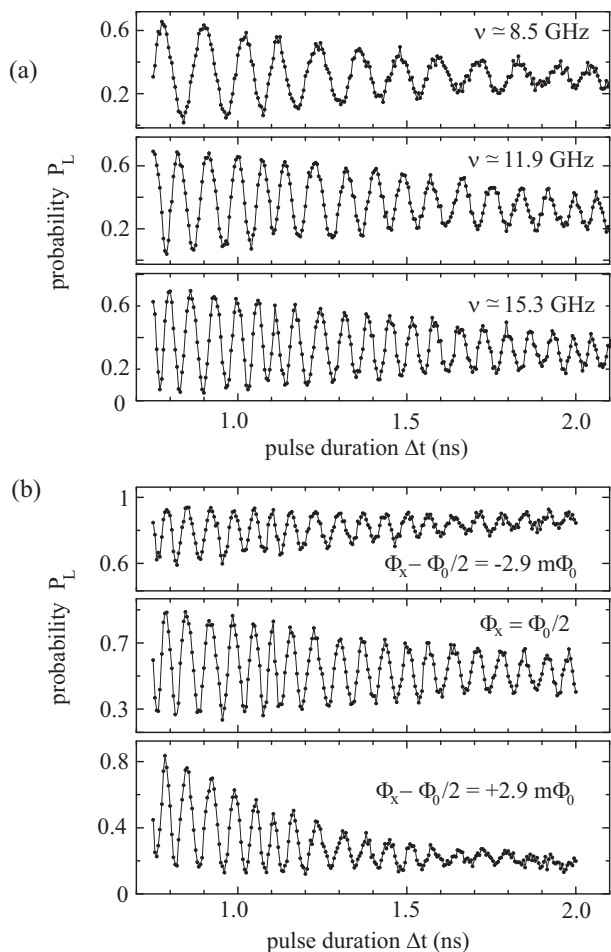


FIG. 4: Probability to measure the state $|L\rangle$ in dependence of the pulse duration Δt for the qubit initially prepared in the $|L\rangle$ state, and for (a) different pulse amplitudes $\Delta\Phi_c$, resulting in the indicated oscillation frequency, and (b) for different potential symmetry by detuning Φ_x from $\Phi_0/2$ by the indicated amount.

supports our interpretation. The fact that a small asymmetry in the potential does not change the oscillation frequency, as shown in Fig. 4(b), is consistent with the interpretation as the energy spacing $E_1 - E_0$ is only weakly affected by small variations of Φ_x . This provides protection against noise in the controlling flux Φ_x .

The measured oscillation decay time of about 2 ns is of the same order as the Rabi oscillations decay and the energy relaxation time T_1 which we measured by using standard microwave π -pulse manipulation on the same device. It is also comparable to the coherence time obtained on similar devices fabricated using the same technology [17], suggesting that coherence is not limited by the manipulation procedure reported in this paper. We believe that the decay time of the reported high-frequency coherent oscillations can be increased by two orders of magnitude by reducing the area of the JJs and using an appropriate dielectric instead of SiO_2 as insulating material in

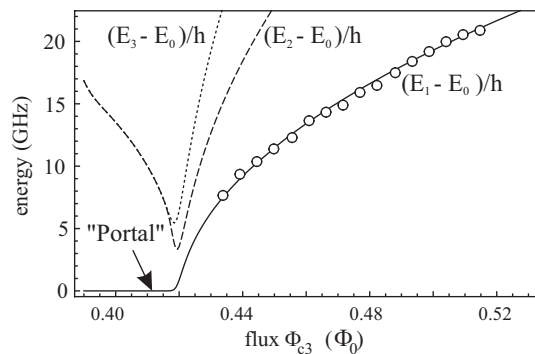


FIG. 5: Calculated energy spacing of the first (solid line), second (dashed line) and third (dotted line) energy levels with respect to the ground state in the single well potential, plotted vs. the control flux amplitude Φ_{c3} . Circles are the experimentally observed oscillation frequencies for the corresponding pulse amplitudes.

the junction fabrication [18].

We note that a similar qubit manipulation procedure has been reported by Koch et al. [5], demonstrating Larmor oscillations in a flux qubit coupled to a harmonic oscillator. It should be emphasized that, in our case, the oscillator is not required, which simplifies the realization of the qubit circuit. Moreover, in contrast to Ref. [5], our approach provides a *wide range tunability* of the frequency of coherent oscillations. This allows for a variety of quantum gates by manipulating both duration and amplitude of the flux pulses, and moreover is important concerning the realization of a controllable coupling between qubits or quantum busses such as resonant cavities.

In conclusion, we presented the coherent manipulation of a flux qubit without using microwaves. The reported approach seems particularly promising for the realization of circuits with many qubits, and it appears to be well suited for integration with RSFQ control electronics [19]. The benefits of the reported system are the possibility of *in situ* tuning the frequency of oscillations and their insensitivity to small changes in the potential symmetry. The high frequency of oscillations allows for very fast qubit gate operations, and the large energy gap between the qubit states during coherent evolution protects the system from thermal activation to upper energy states. Moreover, the oscillation frequency depends only weakly on the control pulse amplitude $\Delta\Phi_c$, in contrast to the exponential sensitivity of the oscillations in a double well potential [20], which makes the qubit manipulation more reliable.

This work was partially supported by the Deutsche Forschungsgemeinschaft (DFG), the CNR RSTL program and the EU projects RSFQubit and EuroSQIP.

-
- * Electronic address: ustinov@physik.uni-karlsruhe.de
- [1] Y. Nakamura, Y. A. Pashkin, and J. S. Tsai, *Nature (London)* **398**, 786 (1999).
 - [2] J.M. Martinis *et al.*, *Phys. Rev. Lett.* **89**, 117901 (2002).
 - [3] I. Chiorescu *et al.*, *Science* **299**, 1869 (2003).
 - [4] D. Vion *et al.*, *Science* **296**, 886 (2002).
 - [5] R. H. Koch *et al.*, *Phys. Rev. Lett.* **96**, 127001 (2006).
 - [6] A. J. Berkley *et al.*, *Science* **300**, 1548 (2003).
 - [7] Y. A. Pashkin *et al.*, *Nature (London)* **421**, 823 (2003).
 - [8] T. Yamamoto *et al.*, *Nature (London)* **425**, 941 (2003).
 - [9] J.H. Plantenberg *et al.*, *Nature (London)* **447**, 836 (2007).
 - [10] M. A. Sillanpää, J. I. Park, and R. W. Simmonds, *Nature (London)* **449**, 438 (2007).
 - [11] J. Majer *et al.*, *Nature (London)* **449**, 443 (2007).
 - [12] C. Cosmelli *et al.*, *Physica C* **372**, 213 (2002).
 - [13] Hypres Inc., Elmsford, N.Y., USA.
 - [14] A. Lukashenko and A. V. Ustinov, *Rev. Sci. Instr.* **79**, 014701 (2008).
 - [15] M. G. Castellano *et al.*, *Phys. Rev. Lett.* **98**, 177002 (2007).
 - [16] R. H. Koch *et al.*, *Phys. Rev. B* **72**, 092512 (2005).
 - [17] J. Lisenfeld *et al.*, *Phys. Rev. Lett.* **99**, 170504 (2007).
 - [18] J. M. Martinis *et al.*, *Phys. Rev. Lett.* **95**, 210503 (2005).
 - [19] M. J. Feldman and M. F. Bocko, *Physica C* **350**, 171 (2001); T. A. Ohki, M. Wulf, and M. J. Feldman, *IEEE Trans. Appl. Supercond.* **17**, 154 (2007).
 - [20] F. Chiarello, *Eur. Phys. J. B* **55**, 7 (2007).